

SELECTIVE SURFACES BY CHEMICAL VAPOR DEPOSITION

David D. Allred
Optical Sciences Center
University of Arizona
Tucson, Arizona 85721

ABSTRACT

We report on three chemical vapor deposited (CVD) photothermal stack configurations which combine promising selectivity, economical fabrication and long life expectancy at 500 C operating temperatures. CVD is a versatile and economic technique for thin film deposition in the microelectronics and protective coatings industries. Our group at the University of Arizona has adapted this technology to the preparation of optical thin films. Our earliest configuration, developed in the mid-1970's, was a CVD polycrystalline silicon-on-stabilized silver stack, which achieved longterm stability (1000 hours cycling from room temperature to 500 C in vacuum), high solar absorptance ($\alpha = 0.76$ at 500 C), and low thermal emittance ($e = 0.07$ at 500 C). Recently, we have developed two other configurations which employ new CVD materials and which appear to be superior to our original silicon-on-silver stacks. One stack configuration consists of a carbon stabilized CVD amorphous silicon absorber layer antireflected with silicon nitride and deposited on CVD thin film molybdenum. Non-optimized stacks have been developed with absorptances of more than 0.75 and emittances of less than 0.03. The optical properties of these coatings were not degraded after 500 hours of anneal at 500 C in air. In our third configuration, a single material functions both as solar absorber and infrared reflector. We have termed this material "black molybdenum". When black molybdenum is antireflected with silicon nitride, it has a high solar absorptance (greater than 0.91) and a low thermal emittance (approximately 0.11), based on room temperature reflectance. The α and e of these coatings were unchanged after 1000 hours of anneal at 500 C in a 1 mm Hg vacuum. We continue to optimize material properties and stack design to maximize solar absorptance, minimize thermal emittance, and insure stability at operating temperatures.

SELECTIVE SURFACES BY CHEMICAL VAPOR DEPOSITION

David D. Allred
Optical Sciences Center
University of Arizona
Tucson, Arizona 85721

I. Introduction

I.1 Overview

The remarkable growth of solar energy technology over the past six years has created a demand for novel optical coatings. The total efficiency of a solar energy system will critically depend on its reflecting, absorbing, and transmitting components. During this recent period, our group at the University of Arizona's Optical Sciences Center has focused on spectrally selective surfaces. We have developed a novel technology based on chemical vapor deposition (CVD) for fabricating multilayer stacks with the selectivity required for efficient, high-temperature photothermal conversion.¹

We hope to stimulate interest in adapting our laboratory results to larger scale production by briefly describing our recent successes and the potential of CVD in preparing photothermal converter coatings. For two fundamental reasons, this technology merits the interest of the plating and metal coating community:

- 1) CVD, already a mature technology in the microelectronics, tool and protective coatings industries, shows promise as a low cost technique for quickly and uniformly coating the very large areas needed for solar energy conversion.
- 2) Rapid laboratory progress on three high temperature, thin film CVD materials - highly reflective molybdenum, black molybdenum, and stabilized amorphous silicon - have set the stage for production of stable selective stacks.

We report here on multilayer stack configurations that meet four essential requirements for high performance coatings: low thermal emittance, high solar absorptance, economical fabrication, and long life expectancy under 500 C operating conditions. The three different stack configurations we will discuss can be tailored to accentuate any of the four requirements, depending on the application required.

I.2 Chemical Vapor Deposition

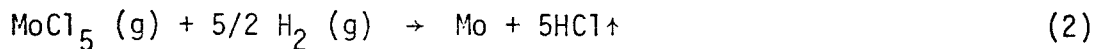
CVD has provided a novel and versatile means of fabricating spectrally selective solar coatings. An example serves to illustrate this process. When a gas mixture containing silane (SiH_4) is brought into contact with a surface hotter than 500 C, sufficient thermal energy to fragment these silane molecules is transferred to them from the surface.² Individual silicon atoms, resulting from the breakup of the silane, remain on the surface as part of a

growing thin film, while hydrogen molecules, also formed, and any undecomposed silane leave the reactor with the carrier gas. The reaction can be written



In short, *vapor* phase molecules receive enough energy from a hot surface for a *chemical* reaction to take place, *depositing* a film, hence the term *chemical vapor deposition*. When a reactant is broken up by heat, it is said to be *pyrolytically* decomposed, or *pyrolyzed*. Examples of *pyrolytically* deposited films for our selective coatings include the deposition of silicon from silane, as in the above example, and the deposition of molybdenum from molybdenum hexacarbonyl $\text{Mo}(\text{CO})_6$ (Section II.2.1).

When two or more reactants are added to the diluting carrier gas the system becomes more complex. An example is our "chloride process." This involves the reaction between a refractory metal halide, molybdenum chloride, and hydrogen gas; the latter reduces the former, leaving behind highly reflecting molybdenum and evolving gaseous hydrogen chloride:



(see section II.2.2)

A schematic drawing of a typical cold wall CVD reactor appears in Figure 1. The essential elements are the vapor generators for solid and liquid reactants (not shown), the reactant and/or carrier gas cylinders, flow meters to regulate the gas flow, a containment vessel for the reaction zone, a heat source, a substrate, and a susceptor on which it sits. Two basic requirements for producing uniform films by CVD are uniform gas flow and uniform substrate heating.

Two strategies can be employed to achieve uniform heating. They are distinguished by the wall temperature of the reaction vessel. The walls in a hot wall reactor have the dual role of containing the reactants and heating the substrates placed within the reactor. Hot wall reactors can be heated by resistance heaters or by radio frequency generators. We employ cool wall reactors; power from the external heating source is transmitted directly through the walls of the reaction vessel to a susceptor upon which the substrates are placed. Heating is localized at the susceptor so the reactor walls remain relatively cool. The susceptor is more massive than the substrates and acts not only as a target for incoming power, but also as a heat reservoir. In our reactor, the susceptor is a graphite block coated with silicon carbide.

In our depositions of silicon compounds from silane and molybdenum from molybdenum carbonyl, the susceptor is heated by high intensity lamps placed outside the clear walled reaction vessel. In fabricating molybdenum thin films by the hydrogen reduction of molybdenum pentachloride (Reaction 2), however, the susceptor is heated by a radio frequency power source.

As in electroplating, the substrate in CVD plays a pivotal role in film formation. In electroplating, the substrate discharges the ions which form the coating. In CVD, the substrate must provide the activation energy and

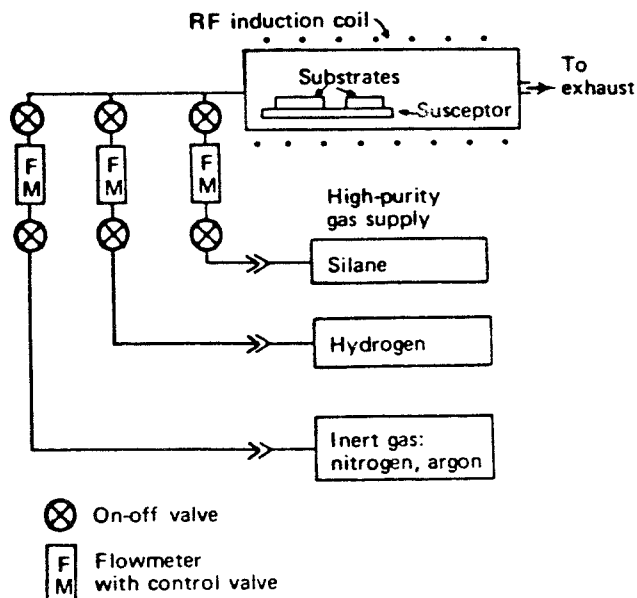


Figure 1. A schematic drawing of a typical inductively heated CVD reactor.

may often act as an active site for the chemical reactions which deposit the film.³ While the substrate is necessarily hot in CVD, it need not be electrically conductive as required by electroplating.⁴ The high deposition temperatures needed by CVD pose problems of mismatched thermal expansion coefficients, agglomeration, interdiffusion, erosion of the substrate by the reactant gas (ablation), and interaction of component layers. Therefore, for certain CVD applications, some substrates and component layers are completely unsuitable, while others may be used only if passivated prior to deposition of the next layer.⁵

On the other hand, high fabrication temperatures prescreen CVD selective surfaces against failure at operating temperature and in many cases improve the quality of the films.⁶ For example, high temperatures during deposition or anneal are essential for the achievement of high reflectance in molybdenum thin films.

A large number of chemical reactions can be harnessed by CVD, making it a very flexible process. Moreover, doping or alloying of films is straightforward in CVD, since additional reactants can be uniformly mixed in the carrier gas stream, although differences in deposition rates among reactants can complicate the process. Refractory metals, characterized by low volatility and high chemical activity, are especially suited to CVD, as are some compounds whose low stability makes them difficult to deposit by evaporation or sputtering. Lastly, very pure films can be deposited by CVD without resorting to the very high vacuums required by the physical vapor deposition (PVD) methods of sputtering or evaporation.

Electroplating, based on the flow of current through a substrate, requires that the substrate be conducting. This is a strong constraint in selective surface development, in that the use of insulating substrates and/or thin films is necessary for many applications. For example, some collector designs require coated glass elements, and many selective surfaces operate more efficiently with antireflection coatings which are made of insulators such as silicon nitride.

Coating rates as high as 1500 $\mu\text{m}/\text{hour}$ have been reported for CVD.⁷ However, in the long run, the important quantity for large scale selective surface production will not be rate but rate times area coated. The vital advantage of CVD over PVD is that once gas flow conditions are optimized for the geometry of the substrate which must be coated, very large areas can be coated in a single deposition.⁸ In the tool and microelectronic industries, areas on the order of 10^4 cm^2 on many small pieces are routinely coated by CVD at one time. In the processes developed at the Optical Sciences Center, deposition rates are between 1 and 10 $\mu\text{m}/\text{hour}$,^{9,10} more than adequate for selective stacks. For example, even at this slow deposition rate, only a few minutes are required to fabricate the absorber layer; these layers are thin, usually less than the wavelength of visible light, in order to exploit interference effects to maximize solar absorptance.

CVD can be carried out at pressures ranging from considerably above atmospheric down to 1 $\mu\text{m Hg}$. Of course, pressure is a parameter which must be optimized to achieve high purity and uniformity of the resulting films. Coating is simplified and costs can be reduced by avoiding non-ambient pressures. All of the selective surfaces made in our laboratory are deposited at ambient pressures. Therefore, long flow-through ovens could be built for the large scale deposition of our coating on pipes and flat plates.⁶ As an alternative to batch production in PVD systems requiring large, expensive diffusion pumps, CVD may provide considerable savings in equipment and time.

When deposition parameters are properly chosen, CVD has greater throwing power, or ability to coat objects of complex shapes with uniform films, than does electroplating or evaporation.⁴ The appearance of unusual concentrator, absorber, and boiler designs may give throwing power increasing importance. Summing up all of the above considerations, we expect to see a growing interest in CVD technology, especially in the area of coatings for solar energy converters.

I.2 Optical Properties

In the conversion of solar radiation to heat, the optical properties of surfaces intercepting the solar flux determine the upper limit of the system's conversion efficiency.¹¹ The desired optical characteristics of a photothermal converter are high absorption over the solar emission spectrum combined with low reradiation loss across the thermal infrared range. Thus, the absorption spectrum of the converter must approximate a step function of wavelength with strong absorption for short wavelengths and very weak, or no, absorption for long ones. The exact location of the step in the absorption profile depends on the conditions of solar flux concentration and the operating temperature.

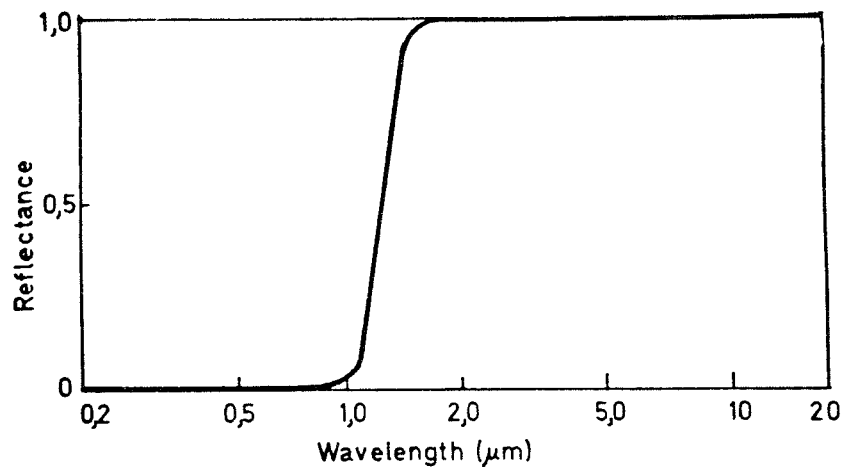


Figure 2. Ideal spectral profile of a photothermal converter.

To quantify the selectivity of our stacks and to compare them with those prepared by other methods, I will briefly define the quantities "solar absorptance" and "thermal emittance" and describe our procedure for their determination:

Solar absorptance, a , is the ratio of the insolation absorbed by a surface to the total insolation incident on that surface, where the insolation must be known as a function of wavelength.

Thermal emittance, $e(T)$ is the ratio of the energy radiated by a surface at a temperature T to that radiated by a blackbody at the same temperature. Both values are evaluated over the hemisphere above the surface.

If possible, the measurements should be made with the surface at operating temperatures. Unless otherwise indicated, however, our calculations of solar absorptance are based on room temperature hemispherical absorptances $a_h(\lambda)$, according to the formula

$$a = \frac{\int_0^{\infty} a_h(\lambda) \mathcal{H}(\lambda) d\lambda}{\int_0^{\infty} \mathcal{H}(\lambda) d\lambda} \quad (3)$$

where an Air Mass 2 solar spectrum is used for the insolation $\mathcal{H}(\lambda)$. Our thermal emittances are computed by the formula

$$e(T) = \frac{\int_0^{\infty} \epsilon(\lambda, T) \mathcal{E}_{bb}(\lambda, T) d\lambda}{\int_0^{\infty} \mathcal{E}_{bb}(\lambda, T) d\lambda} \quad (4)$$

where $\mathcal{E}_{BB}(\lambda, T)$ is the blackbody emission for temperature T .

If it is assumed that the samples are opaque and Kirchoff's Law is valid, the absorptance, $\alpha(\lambda)$, and the emittance $\epsilon(\lambda, T)$, can be approximated by $1-R(\lambda)$, where $R(\lambda)$ is the hemispherical reflectance. Although the evaluations of the solar absorptance in our results are actually based on hemispherical reflectance measurements, it should be noted that within the precision of the measurement the same values are obtained for specular reflectance. The thermal emittances quoted in this paper are based on specular reflectance measurements, giving an upper limit for e , so that the actual thermal emittance may be even smaller. Except for measurements of the silicon-on-silver stacks which were made at 500 C, reflectance measurements were made at 20 C.

To compare the solar absorptance of different absorber materials, it is helpful to plot absorptance against a suitable function of the wavelength such that equal increments along the abscissa correspond to equal fractions of the solar flux (see Fig. 9 and Section II.4). The advantage of such a "distorted wavelength plot" is that solar absorptance can be derived by planimetry of the area beneath the curve with the area of the entire graph representing 100%.¹²

The function which relates the wavelength and the distance along the abscissa is

$$x(\lambda') = \frac{b \int_0^{\lambda'} \mathcal{H}(\lambda) d\lambda}{\int_0^{\infty} \mathcal{H}(\lambda) d\lambda} \tag{5}$$

where b is a scaling factor and, as before, \mathcal{H} is the solar flux. Distorted wavelength plots can also be prepared for determining the emittance at a given temperature given the reflectance spectrum.

Our approach to spectral selectivity has been based on an absorber-reflector tandem, which contains three elements: an absorber layer, which captures the solar flux but which becomes transparent in the thermal infrared, a reflector layer which underlies and essentially looks through the absorber layer to lower the stack's emittance, and an antireflection layer which overlies the absorber and reduces front surface reflection in the stack.

Recently, we have begun to combine the functions of the absorber and reflector in a remarkable material we call black molybdenum (Section II.5). In a parallel development, we have begun combining the functions of the absorber and antireflection layers by making the silicon absorber thin enough so that interference effects between the absorber, the antireflection layer, and the molybdenum add to the absorption. The optimum stack configuration for a particular application will depend on the relative importance of emittance, absorptance, durability, and cost. Fortunately, the optical properties are proving to be amenable to manipulation, so that such optimization appears to be practical.

CROSSSECTION OF THE CONVERTER STACK

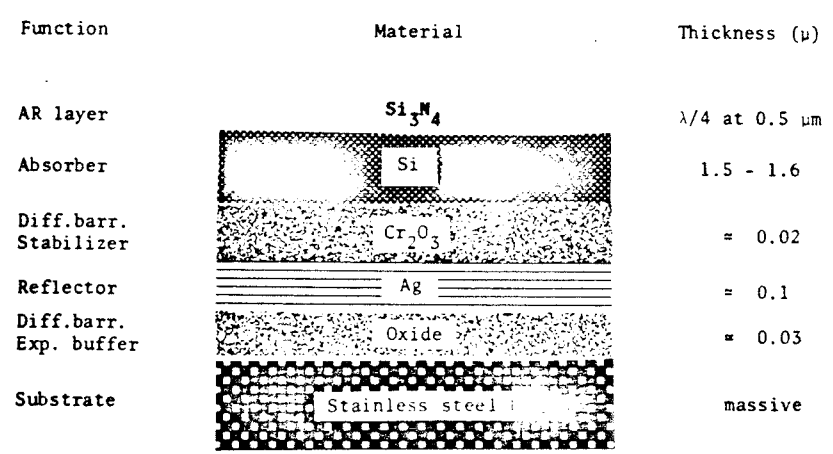


Figure 3. Cross-section and functions of the component layers of a spectrally selective stack for use in high temperature photothermal solar energy conversion.¹

II. CVD Solar Materials and Stack Configurations

II.1 Silicon-on-Silver Coating

Figure 3 shows the design of the first selective surface developed in our laboratory. The essential elements were a suitable antireflected absorber layer (CVD polycrystalline silicon) deposited on a silver reflector layer deposited, in turn, on an oxidized stainless steel substrate. The spectral selectivity was derived from the absorber-reflector tandem principle: the silicon strongly absorbs the solar flux but becomes transparent in the infrared, allowing the highly reflective silver layer below to determine the entire stack's emittance.

Our program developed stacks which could be reproducibly fabricated and which showed noteworthy selectivity. Figure 4 shows the reflectance profile of the state of the art stack at 20 C and 500 C. The solar absorptance and the infrared emittance at 500 C as calculated from the reflectance measured at 500 C are 0.76 and 0.067, respectively. Free carrier absorption is acceptably small in the CVD silicon absorber. We stabilized the silver reflector layer against interdiffusion with adjacent layers and against morphological changes which would otherwise occur during deposition of the rest of the CVD stack or during sustained operation at 500 C. The optical performance of these stacks did not deteriorate when stacks were cycled several thousand times to 500 C in a roughing pump vacuum. Total annealing time exceeded 1000 hours. Sample sets annealed at 700 C in vacuum for several hours lost less than 2.5% of their infrared reflectance.

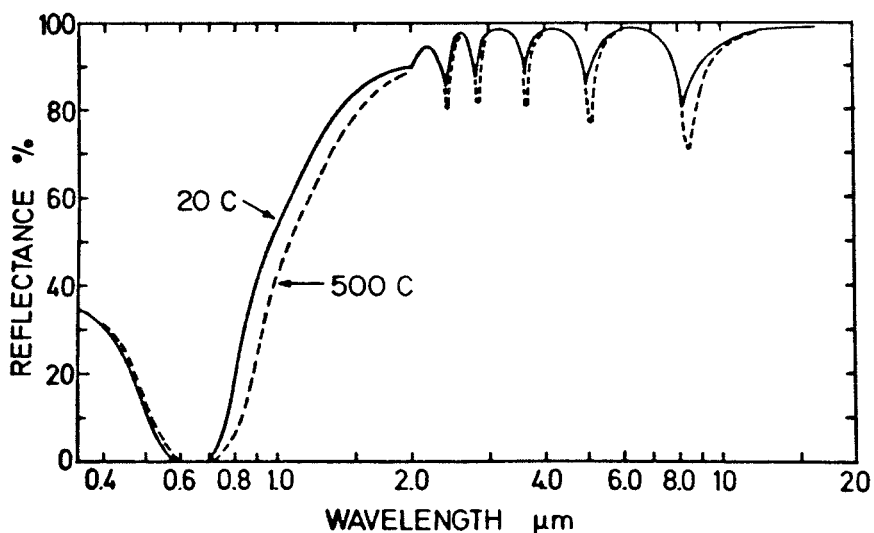


Figure 4. The spectral reflectance of a Si-Ag sample measured at temperatures of 20 C and 500 C. (In the region of rapidly oscillating fringes between 0.7 and 2.0 μm , the effective coating reflectance is plotted.) The silicon thickness is 1.75 μm and the silicon-nitride thickness is 0.07 μm .¹

We are no longer developing the silicon-on-silver stack configuration. Since 1977, our goal has been to improve the stack in two ways: by replacing the polycrystalline absorber layer with amorphous silicon and by replacing the silver reflector layer with a CVD refractory metal film. The work has progressed to the point where the new stack configurations produce superior optical performance, possess greater stability at operating temperatures, and will be easier to fabricate because each layer can be deposited by CVD.

II.2 Highly Reflecting Molybdenum Thin Films

Refractory metals such as tungsten and molybdenum were selected to replace the noble metals for several reasons:

1. The infrared reflectivity of the bulk refractory metals competes with that of silver or aluminum. In Table I, we compare the infrared reflectivities and the 500 C emittances (calculated from infrared spectral measurements) of some common reflector materials.
2. Because of their high melting points, agglomeration is not a problem for 500 C applications.⁶
3. Films of molybdenum and tungsten are readily made by CVD.⁴

We also had to deal with several drawbacks to the use of refractory metals:

1. The expense of refractory metals in bulk form is prohibitive, requiring that they be used as thin films.
2. The reflectance of sputtered or evaporated refractory metal films was reported to be lower than that of the bulk metals.^{6,13}
3. The optical properties of such films were not well known
4. Molybdenum and tungsten oxidize at high temperatures and must be passivated (protected) by a suitable overcoat layer. The emittances of the standard passivators, silicide layers of the base metals, are too high to use for solar applications.¹⁴

We have focused on molybdenum and have successfully dealt with these problems; we expect that tungsten, a subject for future research, will behave similarly. Through CVD, we have produced molybdenum films whose infrared reflectance comes within 0.7 of a percentage point of supersmooth, carefully polished bulk samples.¹⁵ Passivation also has been achieved by employing optically acceptable coatings (Section II.2.4). The topmost curve in Figure 5 shows the absolute reflectance of a bulk molybdenum sample. Reflectance of a CVD molybdenum film passivated by a thin layer of silicon nitride approaches this curve to within a few tenths of a percentage point. An unprotected molybdenum film is only slightly lower in reflectance. Both profiles exceed that of a film sputtered in ultrahigh vacuum.¹⁶ All measurements were performed in the high precision absolute reflectometer of the Michelson Laboratory, Naval Weapons Center, China Lake, CA.

TABLE 1. Reflectance at 10 μm and 500 C emittance calculated from room temperature reflectance data. For emittances, the third figure after the decimal point is given for comparison purposes.

Element	Reflectance (10 μm , 20 C)	$e(500 \text{ C})$
Al (a,b)	98.7	0.022
Ag (b,c)	99.5	0.015
Au (b,c)	99.4	0.016
Cu (b)	98.9	0.017
Mo (d)	98.1	0.031
W (e)	98.5	0.030

^a H.E. Bennett, M. Silver, and E.J. Ashley, JOSA 53, 1089 (1963).

^b G. Hass and L. Hadley, AIP Handbook, 2nd Edition, McGraw-Hill, New York, (1963), pp. 6-119.

^c J.M. Bennett and E.J. Ashley, App. Opt. 4221 (1965).

^d A. Klugmann and J.M. Bennett, in Proc. High Power Laser Optical Components and Component Materials Meeting, J.S. Harris and C.L. Strecker, eds., Defense Advanced Research Projects Agency, p. 163 (1977).

M.M. Kirillova, L.V. Nomerovannoya, and M.M. Noskov, Soviet Physics JETP 33 (6), 1210 (1971).

^e L.V. Nomerovannoya, M.M. Kirillova, M.M. Noskov, Soviet Physics JETP 33 (2), 405 (1971).

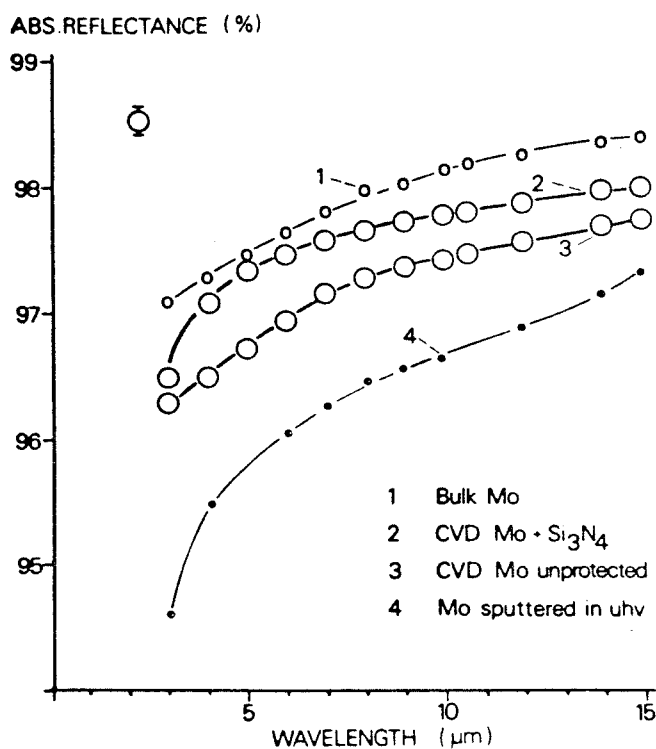


Figure 5. Absolute reflectance of bulk molybdenum (Curve 1), a molybdenum film sputtered in ultra-high vacuum (Curve 4), and two molybdenum films prepared by CVD. Measurements were performed with the High Precision Absolute Reflectometer at the Michelson Laboratory, Naval Weapons Center, China Lake, CA, where the bulk and sputtered samples were also prepared.^{15,16,21}

II.2.1 Molybdenum from the Pyrolytic Decomposition of Molybdenum Carbonyl

One of two techniques for making highly reflecting CVD molybdenum films involves the pyrolytic decomposition of molybdenum carbonyl. The CVD films measured in Figure 5 were prepared using this method. The ideal reaction can be written



We deposited these films at temperatures between 200 and 400 C at one atmosphere with argon carrier gas in a horizontally fed radiatively heated reactor.⁹ Deposition rates were on the order of 0.3 nm/second at 300 C on quartz and nickel substrates. Attempts to work above 400 C at one atmosphere result in gas phase decomposition and powdery, non-adherent films.¹⁷ Because Reaction 6 will not go to completion at temperatures below 400 C,¹⁸ molybdenum oxycarbide (MoO_xC_y with $x+y \approx 1$), rather than pure molybdenum, is deposited. The measured infrared reflectance of this film is considerably inferior (87% of Al at 10 μm) to that of bulk molybdenum.¹⁹ The molybdenum hexacarbonyl

was purchased from the Alfa Division of the Ventron Corporation. It contains as impurities the other two elements in the same column of the periodic table as molybdenum: tungsten and chromium. As a result, our films contain about 1 at.% tungsten and 2 at.% chromium.²⁰

When subjected to a post-deposition anneal in a flowing hydrogen-containing atmosphere (90% He/10% H₂) at temperatures between 750 and 1000 C, the films came within 0.7% of the reflectance of bulk, supersmooth molybdenum.²¹ During this anneal, electrical resistivity falls and grain size grows fifty-fold to approximately 0.5 μm. The molybdenum oxycarbide x-ray lines are replaced by body-centered cubic (bcc) molybdenum x-ray diffraction lines, and most of the carbon and oxygen leave the film.^{21,22} The fact that the annealed film still contains carbon and oxygen is important. For a strongly reactive material such as molybdenum, a realistic technology must tolerate some impurities. It is therefore encouraging that the higher reflectance of annealed CVD molybdenum films is not necessarily tied to very high purity.²³

Table 2 compares conductivity and reflectance values for unannealed and completely annealed films with those of bulk molybdenum. The essential function of hydrogen in the anneal step seems to be to retard oxidation of the molybdenum during the anneal.²⁴

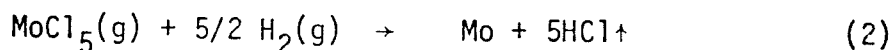
TABLE 2. Thickness, electrical resistivity at 20 C, and absolute reflectance at 10 μm of an as-deposited film, an annealed film, and supersmooth bulk molybdenum

Sample	Thickness (μm)	Resistivity at 20 C (μΩ·cm)	Absolute Reflectance at 10 μm (%)
As-deposited	0.154 ± 0.006	250 ± 25	85.0 ± 1.0
Annealed	0.134 ± 0.007	9 ± 2	97.4 ± 0.1
Bulk Mo	---	5.7 ^a	98.1 ± 0.1

^aHandbook of Chemistry and Physics, 52nd Edition, The Chemical Rubber Co., Cleveland, Ohio, 1971, p. E-72.

II.2.2 Molybdenum from the Hydrogen Reduction of Molybdenum Pentachloride

Reaction 2 above,

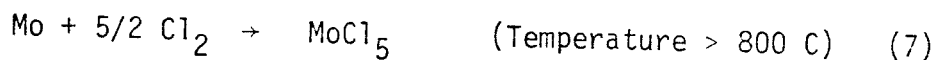


can deposit molybdenum if relatively pure molybdenum carbonyl is used at deposition temperatures above 500 C.²⁵ Some care must be taken with the molybdenum

pentachloride. The presence of oxygen or water vapor would lead to the formation of oxychlorides, which are also reduced by hydrogen, resulting in the inclusion of oxygen in the films. To minimize contamination of the molybdenum pentachloride powder, the source generator is loaded in a glove box under dry nitrogen. Depositions in this system are usually performed at atmospheric pressure in a flowing gas mixture of 10% hydrogen in argon at temperatures ranging from 500 C to 750 C. The inductively heated reaction chamber is horizontal and incorporates pyrex lines and ground glass joints. Molybdenum thin films deposited at 750 C from molybdenum pentachloride exhibit infrared reflectances equaling those of the best annealed films discussed above. These highly reflecting films exhibit bcc x-ray diffraction patterns and are as pure as the fully annealed films produced by the carbonyl process.²⁴

II.2.3 Comparison of Carbonyl and Chloride Processes

The chloride process may be the preferred method for large-scale production. First, it is a less complicated technique. Being a single step procedure, there is no need for a post-deposition anneal, and, although the deposition temperature is higher than that used in the carbonyl process, it is lower than the temperature required in the carbonyl process's annealing step. This is particularly important for molybdenum films deposited on low chrome steel, which has a ferritic to austenitic phase transformation at approximately 725 C. The resultant volume change in the steel substrate during the annealing of a carbonyl process molybdenum film may destroy the optical coating. Finally, the chloride process promises to be more economical than the carbonyl process. In large quantities, it is much cheaper to buy molybdenum and chlorine and combine them in situ via



than to purchase molybdenum chloride. On the other hand, the reactant needed for the carbonyl process, molybdenum hexacarbonyl, cannot be directly produced from molybdenum, but must be purchased or produced from molybdenum pentachloride.

One disadvantage of the chloride process for some substrates and applications, however, is the release of highly corrosive hydrogen chloride. In fact, it is not possible to deposit molybdenum directly onto steel using this process unless the steel first receives a coating, such as nickel, to prevent its chemical erosion.⁵

II.2.4 Passivating the Molybdenum Reflector Against Oxidation

While molybdenum resists the agglomeration and pinhole formation that affects silver, it is subject to a serious degradation mechanism that must be blocked: oxidation. For solar energy applications, we have found this problem not to be insuperable. Our recent work indicates that molybdenum films overcoated with a 25 nm thick silicon nitride film are protected from oxidation while retaining their infrared reflectance, even when exposed to open air at 500 C for several hours.¹⁴ The emittance of these films is not increased by the passivation.

Recently, we also discovered that if the thickness of the passivation layer is increased to 75 - 110 nm, oxidation is slowed even further with no loss of infrared reflectance. Thin film CVD molybdenum samples passivated with 110 nm of silicon nitride have maintained their high infrared reflectance for over 750 hours annealing at 500 C in air. Further, we have found that the stack's absorber layer can also protect the molybdenum film from oxidation. We have lifetime tested solar stacks composed of highly reflecting thin film molybdenum overcoated with a thin (approximately 100 nm) silicon layer antireflected with silicon nitride. These were tested in air for 500 hours at 500 C without showing degradation of optical performance. Accelerated lifetime tests involving passivated molybdenum and complete stacks continue.²⁶

II.3 Amorphous Silicon Absorber Layers

While the very highly reflecting molybdenum which we have prepared by CVD can presumably be combined with many types of absorber layers to produce selective surfaces, we have focused on silicon. Silicon has been a favored candidate for the absorber material, as its absorption edge falls approximately between the solar spectrum and the thermal reradiation,²⁷ and its linear expansion coefficient ($3 \times 10^{-6}/^{\circ}\text{C}$) is very similar to those of molybdenum and tungsten ($5 \times 10^{-6}/^{\circ}\text{C}$ and $4.5 \times 10^{-6}/^{\circ}\text{C}$, respectively),²⁸ lending interfacial stability to the coating.

II.3.1 Amorphous Silicon

In the silicon-on-silver stacks discussed above, the absorber was polycrystalline silicon. Research is now underway to improve the moderate solar absorptance of these converter stacks by replacing the crystalline silicon absorber with a layer of amorphous silicon stabilized against crystallization by alloying with carbon. This would eliminate the problems posed by the polycrystalline silicon, which has a shallow absorption edge allowing too many near-infrared solar photons to pass through unabsorbed.^{2,29}

It has long been known that the absorption profile of amorphous silicon is superior to that of polycrystalline silicon with respect to steepness and spectral position, thereby providing larger solar absorptance.³⁰⁻³² Sputtered or evaporated amorphous silicon, however, crystallizes at 550 C.³³ Not only is the loss of absorption disadvantageous, but the volume changes upon crystallization could destroy the stacks containing amorphous silicon. The converter surfaces would have too short a lifetime at the operating temperatures necessary for reasonable Carnot efficiency. As a consequence, it initially appeared that the silicon phase having superior optical performance had to be ruled out on the basis of insufficient temperature stability.

II.3.2 CVD Amorphous Silicon

Chemical vapor deposited amorphous silicon differs from the evaporated or sputtered material. Incomplete decomposition of the silane molecule leads to the incorporation of hydrogen into the growing film. The resultant material, which contains between 0.2 and 0.7 at.% hydrogen, does not crystallize as rapidly as its sputtered or evaporated counterparts. Detailed studies show that crystallization in amorphous silicon is a gradual process that depends on length and temperature of anneal and proceeds exponentially at higher temperatures. With this in mind, a "crystallization temperature" of 680 C for CVD amorphous silicon can be assigned for comparison with the crystallization temperature of 550 C previously observed for sputtered or evaporated amorphous silicon films.³⁴

In spite of this improvement, the thermally activated crystallization kinetics of CVD amorphous silicon implies that a converter operated at 500 C would survive at the most a few years before progressive crystallization of the absorber layer destroyed the stack. The coincidence of increased resistance to crystallization with the presence of hydrogen in amorphous silicon suggested that intentional doping could further retard the crystallization of CVD amorphous silicon. One constraint of this search was that the doping cannot adversely affect the optical properties of the non-intentionally doped amorphous silicon.

II.3.3 Doped Amorphous Silicon

Our group is presently studying the effects of doping with C, N, B, or Ge on the crystallization behavior and optical properties of CVD amorphous silicon.^{10,35} Carbon has received the most attention, because the solar absorptance of the alloyed material exceeds even that of the non-intentionally doped material. In addition, in alloys of silicon with carbon or nitrogen, the crystallization is retarded to a point where stacks operating at temperatures in excess of 700 C can be expected to survive for decades.

In Figure 6 are plotted the absorption coefficients of films doped with carbon at various levels of concentration. Note that the gain in solar absorptance is most pronounced for films doped with 18 at.% C. In films doped with a higher concentration, the profile of the absorption coefficient drops below that of the non-intentionally doped material above photon energies of 1.6 eV.

The intensity of the Si{111} x-ray diffraction peak is plotted as a function of the length of the anneal relative to that of a standard CVD polycrystalline film in Figure 7. The non-intentionally doped film annealed at 650 C starts to crystallize after less than two hours, in agreement with the results of Janai and his colleagues.³⁴ In contrast, a film doped with 18 at.% C withstands an anneal at 950 C for up to ten hours before substantial crystallization starts.

In order to describe the crystallization process in quantitative terms, we define the "crystallization time" as the time when the inflection point occurs in profiles such as those given in Figure 7. Such a point was observed for all the dopants studied in sufficient detail. Plotted as a function of reciprocal absolute temperature, the logarithms of the crystallization times

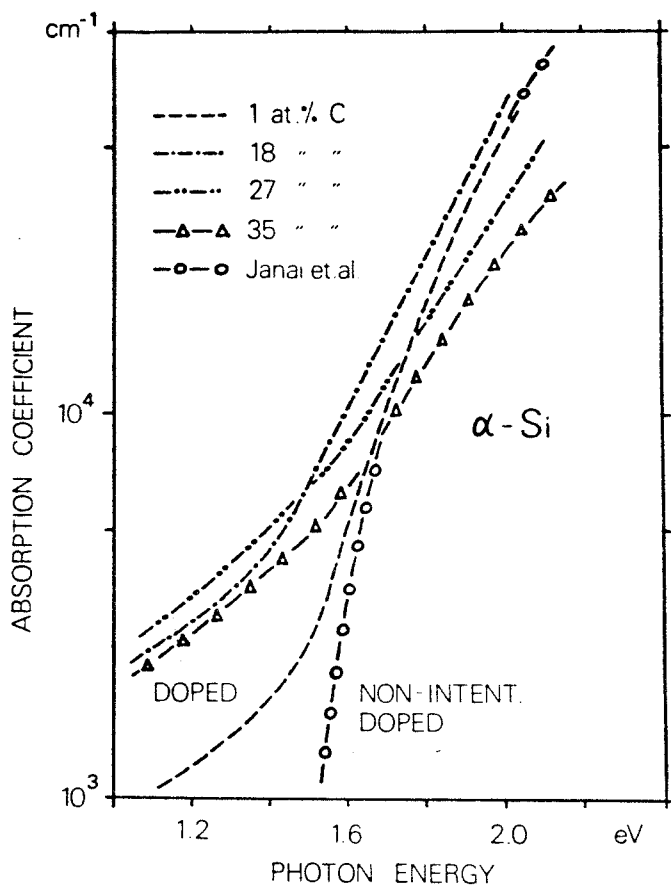


Figure 6. Absorption coefficient as a function of photon energy for CVD amorphous silicon doped with various concentrations of carbon.^{10,35}

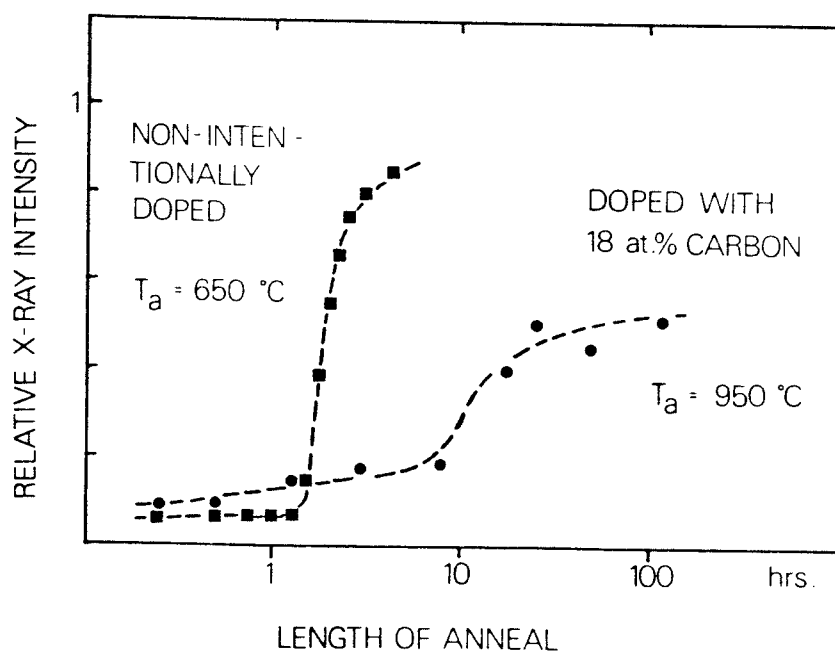


Figure 7. Intensity of the Si{111} diffraction peak (normalized to the peak heights observed for a standard CVD polycrystalline sample) vs. annealing time, T_a .^{10,35}

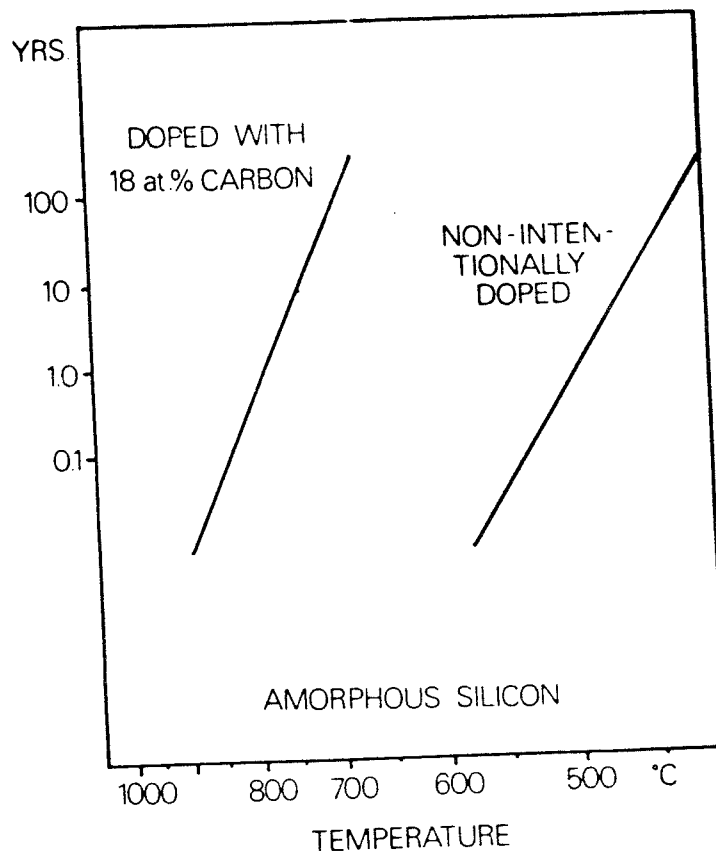


Figure 8. Crystallization time vs. anneal temperature for CVD amorphous silicon for 18 at.% carbon.^{10,35}

fall on a straight line. This suggests expressing the rate of crystallization in terms of an Arrhenius equation. The slope and the intercept with $1/T = 0$ of the profiles plotted in Figure 8 determine in this equation the activation energy and the pre-exponential factor, respectively.

The straight line on the left in Figure 8 represents the most conservative assessment of the data collected on the crystallization of amorphous silicon doped with 18 at.% carbon. The straight line on the right is based on the data reported by Janai and his colleagues for the crystallization of non-intentionally doped amorphous silicon.³⁴

From our research we have learned the following:

1. Carbon and nitrogen both retard crystallization, while boron does not.
2. For a given temperature of anneal the retardation is most effective for a high concentration of the dopant.
3. For a given carbon concentration, crystallization proceeds faster at higher temperatures of anneal, as expected.

From the data in Figure 8, we conclude that the structural lifetime of a photothermal converter surface that uses carbon-stabilized silicon as the absorber would be on the order of several decades, if the surface is continuously

operated at 700 C. Operation at 650 C would extend the crystallization time to several hundred years. If this extrapolation on the basis of the Arrhenius equation is correct, the retardation of the crystallization by carbon doping contributes significantly to the structural lifetime of an amorphous silicon solar absorber.

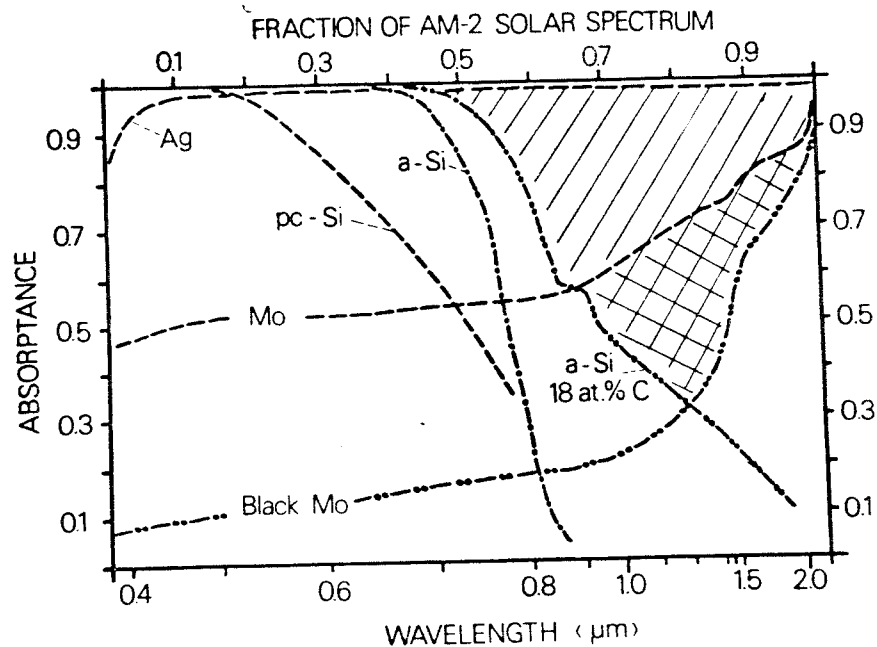


Figure 9. Double-pass absorptance through a 1 μm thick sample of polycrystalline silicon (pc-Si)³⁴, non-intentionally doped amorphous silicon (α-Si)³⁴ and stabilized amorphous silicon (α-Si, 18 at.% C) plotted on a distorted λ-plot. Superimposed are the reflectances of silver, CVD molybdenum²¹, and black molybdenum²⁴. Shaded and crosshatched areas qualitatively correspond to the gain in absorptance over a silver reflector. Note that kinks in the curves are caused by irregularities of the distorted λ-plot that represent absorption bands in the solar spectrum.¹⁰

II.4 CVD Selective Surfaces Using Amorphous Silicon and Molybdenum

Absorber-reflector tandems based on stabilized amorphous silicon absorbers and highly reflecting molybdenum thin film reflectors are the second configuration of CVD selective surfaces prepared at the University of Arizona. Our group is just beginning the work of stack fabrication using the new carbon-doped amorphous silicon on highly reflecting thin film molybdenum reflectors. Because of differences in optical properties of CVD amorphous

silicon as compared to CVD polycrystalline silicon, on the one hand, and molybdenum as compared to silver, on the other, the solar stacks with the highest α with ϵ less than 0.10 will have an absorber layer about an order of magnitude thinner than the silicon-on-silver stacks developed earlier. The reason for this difference is that, unlike silver, molybdenum is not a broadband reflector. Over the solar spectrum, its reflectance averages about 60%. The rest of the incident radiation is absorbed by the metal. In Figure 9, the reflectance of highly reflective and black molybdenum (Sect. II.5) and silver are plotted against wavelength on a distorted wavelength plot for an Air Mass 2 solar spectrum.

Also shown in Figure 9 are the absorbance profiles derived from

$$A(\lambda) = 1 - \exp[-2 \cdot \alpha(\lambda) \cdot d] \quad (8)$$

for polycrystalline, non-intentionally doped amorphous, and stabilized amorphous silicon (18 at.% C) for a 1 μm thick film. To interpret the areas above the curves in terms of solar absorptance, the reflection loss at the absorber/air interface must be taken into account.

Due to silver's high reflectance in the infrared, photons that pass through the absorber at wavelengths longer than its absorption edge are not absorbed. In contrast to silver's broadband reflectance, some metals and compounds combine moderate reflectance over the solar emission band with high infrared reflectance. Molybdenum, due to its d electrons, is one of these materials.*²¹

The slashed and cross-hatched areas in Figure 9 qualitatively correspond to the gain in absorptance over silver of highly reflective and black molybdenum, respectively. The need for a thin absorber layer is another manifestation of molybdenum's different optical properties. The optical constants of silicon are a better match to molybdenum than to silver.²⁹ The silicon can partially antireflect the metal on which it sits. This antireflection effect of silicon-on-silver stacks does not seriously degrade emittance (note the sawtooth pattern for 2 - 10 μm in Figure 3). For stacks which use the same thickness of silicon (over 1 μm) used in silicon-on-silver stacks, the fringe minima are sufficiently deep, however, to increase thermal emittance to intolerable levels.

Cutting the thickness of the absorber by an order of magnitude pulls the fringes out of the thermal infrared into the solar band. Immediately, the stack emittance decreases to a value closer to that of bare molybdenum and, if the fringes are positioned correctly, the stack absorptance increases. In essence, making the silicon layer thinner causes it to gain a second function. In addition to its role as the absorber layer in an absorber-reflector tandem, it antireflects the molybdenum over the solar spectrum. The silicon layer itself still requires antireflection with silicon nitride and the thickness of these two layers must be jointly optimized to maximize solar absorptance. The α value of non-optimized stacks has exceeded 0.75 and, based on infrared reflectance measurements, the 500 C thermal emittance of the stacks is calculated to be ≤ 0.08 . Future work will be concerned with optimizing the thicknesses to maximize α and minimize ϵ .

*Based on published reflectance data,³⁸ it appears that tungsten may provide greater absorptance than molybdenum. The boundary between moderate and high reflectance is more distinct and tungsten reflects less in the visible. We plan to deposit and study tungsten soon.

It has also been shown feasible to deposit silicon directly onto molybdenum with no destructive effects. Such stacks with an anti-reflection coating of silicon nitride have withstood 500 hours testing in air at 500 C without apparent interdiffusion of the layers or degradation of the molybdenum reflector. In addition, stacks consisting of 1000 Å of carbon-stabilized amorphous silicon on molybdenum without the protection of an anti-reflection layer have withstood 750 hours at 500 C in air with little or no reduction of the infrared reflectance.^{26,39}

II.5 Black Molybdenum: Single Layer Converter?

Bare molybdenum, as evidenced by the distorted wavelength plot in Figure 9, could function in high vacuums as an absorber with an α of 0.37 and an $\epsilon(500\text{ C})$, based on room temperature reflectance, of 0.03. While its solar absorptance is too low for any conceivable use, if the optical properties of bare molybdenum could be altered to enhance absorptance while maintaining a small ϵ value, it could prove very useful for solar applications.

CVD black molybdenum, developed in the past year at the Optical Sciences Center, fulfills this promise.^{3,22} The preparation of black molybdenum is a two step process, involving a deposition followed by an anneal, and thus resembles the preparation of highly reflecting molybdenum films via the carbonyl process. The difference between the two processes lies in the composition of the gas stream during the deposition. Black molybdenum thin films are deposited from molybdenum hexacarbonyl in the presence of an oxygen bleed at 300 C. (The solar absorptance and emittance of the deposited material is a function of oxygen flow rate.) The material is almost entirely fine-grained MoO_2 , as evidenced by TEM, x-ray diffraction, and quantitative microprobe analysis.

The maximum solar absorptance achieved by mid-1979 is about 0.77.²⁴ Unfortunately, emissivity is also very high. Post-deposition annealing in hydrogen decreases the infrared emittance, however, at the expense of also decreasing the visible absorptance of black molybdenum. During this hydrogen anneal, these films lose oxygen, presumably as H_2O , and partially revert to a bcc crystal structure. A thirty minute anneal under a flowing hydrogen containing atmosphere at 1000 C completely reduces black molybdenum. Both the infrared and visible reflectance of these fully annealed black molybdenum films approach that of the highly reflecting films deposited by molybdenum hexacarbonyl without an oxygen bleed. However, high reflectance over the solar spectrum is not desirable, as was pointed out in the previous section. For this reason, our interest in black molybdenum lies in the optical properties that can be obtained by a partial anneal. We have found that during anneal, the infrared reflectance increases more rapidly than the accompanying increase in the visible reflectance. (Contrast Curves 2 and 3 in Figures 10 and 11.) After an anneal of seven minutes at 770 C, we obtain a single layer which exhibits respectable selectivity: $\alpha = 0.74$, $\epsilon(500\text{ C}) = 0.08$ (See Table III and Figures 10, 11).

Recent electron microprobe analysis indicates that partially annealed black molybdenum contains approximately 20 at.% oxygen. The absorption mechanism of black molybdenum is still unknown. We have found that the optical

constants of our CVD silicon nitride match black molybdenum well enough to enable an overcoat of the nitride to antireflect the black film over a wide band in the visible spectrum. The silicon nitride film also passivates the black molybdenum against oxidation. This antireflected black molybdenum represents the third configuration of CVD selective surfaces which our group has developed.

With antireflection, black molybdenum films from a seven minute anneal have attained a solar absorptance of 0.91 and a thermal emittance, as based on the 500 C blackbody profile, of 0.11. The α and e values of black molybdenum and highly reflective molybdenum discussed in Section II.2 are summarized in Table III and in Figures 10 and 11.

TABLE III. α and e of Molybdenum from the Carbonyl Process²⁴

<u>Sample</u>	<u>α (% of Air Mass 2)</u>	<u>e(500 C)</u>	<u>Curve Number in Figures 10,11</u>
Annealed highly reflective molybdenum	0.37	0.03	1
As-deposited black molybdenum	0.77	0.44	2
Annealed black molybdenum (770 C, 7 min.)	0.74	0.08	3
Anti-reflected annealed black molybdenum (770 C, 7 min.)	0.91	0.11	4
Anti-reflected black molybdenum (1000 C, 5 min.)	0.82	0.08	not shown

The thickness of the nitride layer was chosen so that its first interference fringe coincides with the solar peak. The first interference fringe is broad, as Curves 3 and 4 of Figures 10 and 11 show, and successfully anti-reflects black molybdenum over the entire Air Mass 2 spectrum. The dependence of α and e on nitride thickness is being investigated. We are also optimizing the values of α and e of black molybdenum by making systematic changes in the oxygen flow rate during deposition, the anneal temperature, and the length of the anneal. For example, lower emittances are possible, but at the expense of lower absorptances, as shown in the last line of Table III. Our optimization program should lead to an understanding of the absorption mechanism of black molybdenum. These early data for black molybdenum establish it as a single layer, highly selective converter.

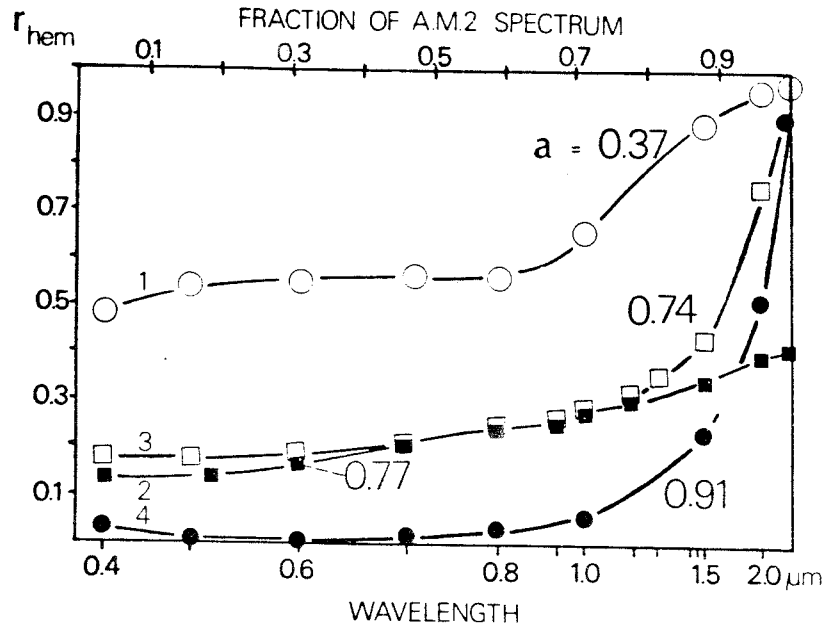


Figure 10. Distorted λ -plot of the solar absorptance a of a set of thin molybdenum films. See Table III for the different treatment of the samples.²⁴

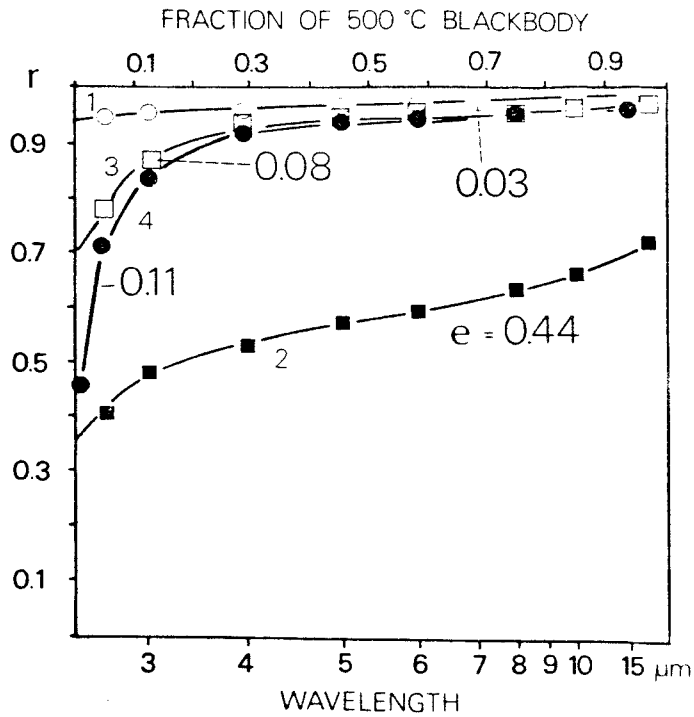


Figure 11. Distorted λ -plot of the thermal emittance e for a blackbody temperature of 500 C for the sample set of Figure 10.²⁴

Antireflected black molybdenum, in addition to its superior optical performance, promises to be stable at high temperatures. During the anneal step, it is exposed to temperatures of 800 C and therefore should not deteriorate rapidly at operating temperatures of 500 C. Preliminary tests have shown this to be the case. The α and ϵ of two antireflected black molybdenum samples have not changed after 1000 hours at 500 C in a vacuum of 1 mm of mercury.³⁹ This indicates that the partially annealed state of black molybdenum is stable over extended periods of time at 500 C without suffering diffusion-related failure. Future tests will be performed in oxygen-bearing atmospheres.

II.6 Comparison of CVD Stacks

In the preceding sections three CVD stack configurations were described. In summary, we present the basic characteristics of the three:

TABLE IV. A Summary of CVD Selective Surfaces

Parameter Investigated	Si-on-Ag ^{1,2,6,40}	Amorphous Si-on-Mo ^{2,9,10,26,29,39}	Antireflected Black Mo ^{3,24,26,39}
α (20 C)	0.72	>0.75	0.91
α (500 C)	0.76	Data not available	Data not available
ϵ (500 C)	0.07	\leq 0.08	0.11
Substrate barrier layer	Native oxide	Under investigation	Under investigation
Reflector layer (thickness)	Evaporated Ag (>0.1 μ m)	CVD molybdenum (>0.2 μ m)	CVD black molybdenum (>0.3 μ m)
Barrier layer	Cr ₂ O ₃	None	None
Absorber layer (thickness)	CVD polycrystalline Si (>1 μ m)	CVD, doped amorphous Si (\approx 0.1 μ m)	None
Antireflection layer (thickness)	CVD Si ₃ N ₄ (\approx 0.07 μ m)	CVD Si ₃ N ₄ (\approx 0.07 μ m)	CVD Si ₃ N ₄ (\approx 0.07 μ m)
Total layers deposited	5 layers	3-4 layers	2-3 layers
Absorption mechanism	Absorber-reflector tandem with interference effects	Absorber-reflector tandem with interference effects	Under investigation
Stack stability	>1000 hours at 500 C in vacuum	>500 hours in air (test continuing)	>1000 hours at 500C in vacuum (tests continuing)
Maturity	Developed	Under development	Under development
Deposition	Not all-CVD technology	All-CVD	All-CVD
Advantages	Adapted to stainless steel substrates	Low emittance probable	High absorptance achieved

III. Future Directions

In addition to the development of new materials and their integration into high-temperature stable photothermal stacks, our Optical Sciences Center group plans to produce a class of CVD thin films whose index of refraction grades continuously within a single layer from that of amorphous silicon (in the visible, $n \approx 4.0$) to that of silicon dioxide ($n \approx 1.5$). By changing the identity and quantity of dopant gas added to the silane-carrier gas mixture as the film grows, the composition of the deposit can be altered in a continuous manner, resulting in a preprogrammed profile of the refractive index. We have already shown, for instance, that by gradually changing the fractional composition of the gas stream, the deposition can go through the sequence: silicon nitride ($n \approx 2.0$) \rightarrow silicon oxynitride (n varies from 2.0 to 1.5) \rightarrow silicon dioxide ($n \approx 1.5$). Such *graded-index profiles* antireflect over a large angular field of view, giving the resulting stack superior performance in concentrating collectors of large optical acceptance angles.⁴¹

There are two other uncompleted tasks that we wish to call to the attention of the coating community. The first is the deposition of a complete stack on the substrates now used in solar collectors. At the present time, only silicon-on-silver stacks have been deposited on metal substrates, which are important for high temperature uses. We are now in the process of adapting the molybdenum deposition to metal substrates. CVD molybdenum is known to form strong bonds to nickel, and it may to other metals.⁵ A study of molybdenum deposition on nickel coated steel and other alloys with and without diffusion barriers is underway. But, as the strengths of our group lie in CVD and optics technologies, we welcome the collaboration of the plating community in investigating the deposition of CVD selective surfaces on appropriate substrates.

We would also like to interest members of the solar coating community in large-scale CVD coating possibilities. It is not premature to consider the deposition apparatus which might be built, albeit that the optimum stack configuration has yet to be determined. CVD selective stacks are composed of two distinct classes of materials, implying that at least two deposition steps will be required. The components of the stacks will be a CVD metal reflector (e.g. of molybdenum) and an absorber and/or antireflection layer containing silicon from silane, in the form of stabilized amorphous silicon and/or silicon nitride.

Our present CVD process can be expanded to production dimensions by either the batch or continuous CVD processes. In the former process, the CVD layers are deposited on the substrate pipe by sequentially introducing the appropriate reactant gases into the deposition chamber. A disadvantage to this technique is that the warm-up and cool-down times of the reaction will probably be much longer than the few minutes required to deposit the entire CVD stack.

Continuous CVD is adapted to long pipes and plates. Since the depositions are done at atmospheric pressure, the whole CVD oven can be an open tube, in principle. In this process, the multilayer stack is built up as the pipe moves through a series of reaction zones, each separated by inert gas curtains. The advantages of this flow-through operation are that substrate-handling and heating energy requirements are minimized.

If CVD technology is to be employed in the large-scale production of selective surfaces, economic feasibility must be shown. Production costs comprise a combination of labor, capital, maintenance, energy, and materials costs. A

careful extrapolation from the experience of the microelectronics and protective coatings industries with CVD will be helpful in determining the overall cost of large-scale CVD applications. Atmospheric CVD fabrication will minimize capital costs. Materials costs for the coatings are also likely to be a modest fraction of the total cost. The highest price in 1977 for molybdenum and silver reflector materials was approximately \$20/kg and \$160/kg, respectively.⁴² The major cost of both the silicon absorber layer and the antireflection layers is the cost of silane. The price of silicon based on the 1979 cost of silane (15 kg cylinder from Matheson) is \$460/kg of silicon. One kg is sufficient to cover a 1,000 square meter area with 0.1 μm of reflector material or with 0.4 μm of absorber, assuming there are no losses.

We see in the successful transfer of CVD technology to the fabrication of spectrally selective surfaces a promising addition to solar conversion technology. The two features under development - greater solar absorptance and simplified fabrication through the use of CVD amorphous silicon and CVD molybdenum - will enhance this potential in the next few years.

IV. Acknowledgements

This article reviews the results of a group effort, describing work undertaken at the Optical Sciences Center of the University of Arizona. Contributors, in alphabetical order, were: D.D. Allred, D.C. Booth, G.E. Carver, E.E. Chain, H.S. Gurev, R.E. Hahn, P. Hillman, M.R. Jacobson, M. Janai, R.D. Lamoreaux, K.D. Masterson, R.H. Potoff, B.O. Seraphin, and R.P. Shimshock.

In addition to previous contracts with the U.S. Department of Energy and its predecessor agencies, the U.S. Energy Research and Development Agency and the U.S. National Science Foundation (RANN), the work is presently supported by the following two contracts:

"Chemical Vapor Deposition of Amorphous Silicon for Photothermal Solar Energy Converters," Department of Energy, Division of Materials Sciences, Office of Basic Energy Sciences, Grant No. ER-78-S-02-4899.

"Chemical Vapor Deposition of Refractory Metal Reflectors for Spectrally Selective Solar Absorbers," Department of Energy, Advanced Technology Branch, Grant No. EY-76-S-04-3709.

The most helpful editorial assistance of Ms. B.J. Manning is gratefully acknowledged.

REFERENCES

1. R.E. Hahn and B.O. Seraphin, J. Vac. Sci. Technol. 12, 905 (1975).
2. D.C. Booth, M. Janai, G. Weiser, D.D. Allred, and B.O. Seraphin, S.P.I.E. Proceedings 161, Optics Applied to Solar Energy IV, 72 (1978).
3. J.J. Cuomo, Proc. 3rd Intl. Conf. on Chem. Vapor Dep., Salt Lake City, Utah, p. 270 (1972).
4. C.F. Powell, J.H. Oxley, and J.M. Blocher, Jr., Vapor Deposition, John Wiley and Sons, Inc., New York, 1966, p. 1, 251-253.
5. J.I. Federer and L.E. Poteat, Proc. 3rd Intl. Conf. on Chem. Vapor Dep., Salt Lake City, Utah, p. 591 (1972).
6. H.S. Gurev and B.O. Seraphin, Proc. 5th Intl. Conf. on Chem. Vapor Dep., The Electrochemical Society, p. 667 (1975).
7. A.M. Schroff, Proc. of 3rd Intl. Conf. on Chem. Vapor Dep., Salt Lake City, Utah, p. 69 (1972).
8. W.A. Brown, T.I. Kamains, Solid State Technology 22, 51 (1979).
W. Kern and G. Schnable, IEEE Trans. on Electron Devices, ED26 (4), 647, (1979).
9. G.E. Carver and B.O. Seraphin, 2nd Ann. Conf. on Absorber Surfaces for Solar Receivers, Boulder, Colorado, 24-25 January 1979.
10. D.C. Booth, D.D. Allred, and B.O. Seraphin, Solar Energy Materials 2 (1/2), to be published.
11. L. Melamed and G.M. Kaplan, J. Energy 1, 100 (1977).
12. L.F. Drummeter and G. Hass, Phys. Thin Films 2, 305 (1964).
13. H.E. Bennett, Semi-Annual Report No. 6, ARPA Order 2175 (May 1975).
14. G.E. Carver, H.S. Gurev, and B.O. Seraphin, J. Electrochem. Soc. 125, 1138 (1978).
15. A. Klugmann and J.M. Bennett, Proc. High Power Laser Optical Components and Component Materials Meeting, J.S. Harris and C.L. Strecker, eds., Defense Advanced Research Projects Agency, p. 163 (1977).
16. P.A. Temple et al., High Energy Laser Mirrors and Windows, Annual Report No. 9, Naval Weapons Center, China Lake, California, TP 5988, p. 18 (Nov. 1977).
17. J.J. Lander and L.H. Germer, Trans. AIME 175, 648 (1948).
18. A.P. Patokin and V.V. Sagalovich, Russian J. Phys. Chem. 50, 3 (1976).
19. G.E. Carver, D.D. Allred, and B.O. Seraphin, S.P.I.E. 161, Optics Applied to Solar Energy IV, 66 (1978).
20. D.D. Allred, 2nd Ann. Conf. on Absorber Surfaces for Solar Receivers, Boulder, Colorado, 24-25 January 1979, presentation.
21. G.E. Carver and B.O. Seraphin, Appl. Phys. Lett. 34, 279 (1979).
22. G.E. Carver, Solar Energy Materials 1(5/6), 1979, to be published.
23. B.O. Seraphin, J. Vac. Sci. Technol. 16 (2), 193 (1979).

24. G.E. Carver, Thin Solid Films, to be published.
25. D.K. Seto, V.Y. Doo, and S. Dash, Proc. of 3rd Intl. Conf. on Chem. Vapor Dep., 1971, p. 659.
26. B.O. Seraphin, Technical Report, Grant No. EY-76-S-04-3709, U.S. Department of Energy, May 1979.
27. D.K. Edwards, J.T. Gier, K.E. Nelson, and R.D. Roddick, Proc. U.N. Conf. on New Sources of Energy, United Nations, New York, 1964, Vol. 4.
28. Handbook of Chemistry and Physics, 58th Ed., 1977-78, p. D-173.
29. D.C. Booth and B.O. Seraphin, Proc. of 2nd Ann. Conf. on Absorber Surfaces for Solar Receivers, Boulder, Colorado, 24-25 January 1979.
30. B.O. Seraphin, Proc. of Symp. on Material Science Aspects of Thin Film Systems in Solar Energy Conversion, Tucson, Arizona, 20-22 May, 1974. NSF-RANN Grant GI-43-795, p. 7 (1974).
31. B.O. Seraphin, J. Jpn. Soc. Appl. Phys. 44, 11 (1975).
32. R.W. Griffith: Sharing the Sun - Solar Technology in the Seventies, Winniped, Canada (1975), Intern. Solar Energy Soc. 6 (1976), p. 205.
33. M.H. Brodsky, M.A. Frisch, J.F. Ziegler, W.A. Lanford, Appl. Phys. Lett. 30, 561 (1977).
34. M. Janai, D.D. Allred, D.C. Booth, and B.O. Seraphin, Solar Energy Materials 1, 11 (1979).
35. D.C. Booth, D.D. Allred, and B.O. Seraphin, Proc. 8th Intl. Conf. on Liquid and Amorphous Semiconductors, Boston, Mass., USA, August 1979. To be published in J. Noncryst. Solids.
36. M.M. Kirillova, L.V. Nomerovann ya, and M.M. Noskov, Soviet Physics JETP 33 (6), 1210 (1971).
37. J.H. Weaver, D.W. Lynch, and C.G. Olson, Phys. Rev. B10, 501 (1974).
38. L.V. Nomerovann ya, M.M. Kirillova, and M.M. Noskov, Soviet Physics JETP 33(2), 405 (1971).
39. Technical Reports, Grant No. ER-78-S-02-4899, U.S. Department of Energy, 1979.
40. H.S. Gurev, R.E. Hahn, and K.D. Masterson, Intl. J. Hydrogen Energy 2, 259 (1977)
41. A. Donnadieu and B.O. Seraphin, J. Opt. Soc. Am. 68, 292 (1978).
42. Metal Statistics: 1978, American Metal Market, Fairchild Publications